

# VIBRATION OF TWO-DIRECTIONAL FUNCTIONALLY GRADED SANDWICH TIMOSHENKO BEAMS TRAVERSED BY A HARMONIC LOAD

Vu Thi An Ninh<sup>1,\*</sup>, Le Thi Ngoc Anh<sup>2,3</sup>, Nguyen Dinh Kien<sup>3,4</sup>

<sup>1</sup>University of Transport and Communications, 3 Cau Giay, Ha Noi, Viet Nam

<sup>2</sup>Institute of Applied Mechanics and Informatics, VAST, 291 Dien Bien Phu, Ho Chi Minh City, Viet Nam

<sup>3</sup>Graduate University of Science and Technology, VAST, 18 Hoang Quoc Viet, Ha Noi, Viet Nam

<sup>4</sup>Institute of Mechanics, VAST, 18 Hoang Quoc Viet, Cau Giay, Ha Noi, Viet Nam

\*Email: [yuthianninh@utc.edu.vn](mailto:yuthianninh@utc.edu.vn)

Received: 30 March 2020; Accepted for publication: 12 July 2020

**Abstract.** Vibration of two-directional functionally graded sandwich (2D-FGSW) Timoshenko beams traversed by a harmonic load is investigated. The beams consist of three layers, a homogeneous core and two functionally graded skin layers with the material properties continuously varying in both the thickness and length directions by power functions. The conventional functionally graded sandwich beams are obtained from the present 2D-FGSW beams as a special case. A finite element formulation is derived and employed to compute the vibration characteristics of the beams. The obtained numerical result reveals that the material distribution and the layer thickness ratio play an important role on the natural frequencies and dynamic magnification factor. A parametric study is carried out to highlight the effects of the power-law indexes, the moving load speed and excitation frequency on the vibration characteristics of the beams. The influence of the aspect ratio on the vibration of the beams is also examined and discussed.

**Keywords:** 2D-FGSW beam, moving harmonic load, vibration analysis, dynamic magnification factor, finite element formulation.

**Classification numbers:** 5.4.2, 5.4.5.

## 1. INTRODUCTION

Functionally graded material (FGM), initiated by Japanese researcher in mid-1980s [1], has wide application in automotive and aerospace industries. This material is recently employed in the fabrication of sandwich structural elements to improve the performance of the structures. Functionally graded sandwich (FGSW) structures with smooth variation of material properties overcome the problem of layer separation and stress concentration as often seen in traditional sandwich structures. Vibration analysis of FGSW beams, the topic discussed herein, has drawn

much attention from researchers. Many investigations on free and forced vibration of sandwich beams are available in the literature, the contributions that are most relevant to the present work are briefly discussed below.

Based on the discrete Green function, Sakiyama *et al.* [2] derived the characteristic equation of the free vibration of the sandwich beam with an elastic or viscoelastic core. Apetter *et al.* [3] considered static bending of the sandwich beams with a FGM core using different beam theories. The element free Galerkin and penalty methods were used by Amirani *et al.* [4] in vibration analysis of sandwich beam with an FGM core. Free vibration of the sandwich beam with a functionally graded syntactic core was considered by Rahmani *et al.* [5] using a high-order sandwich panel theory. Bending, buckling and free vibration of the FGSW beams were studied in [6, 7] using various shear deformation theories. Free vibration and buckling analyses of FGSW beam were also considered by Vo *et al.* [8] using a quasi-3D finite element model.

The beam under moving loads is an important problem in practice, especially in the transportation field. Investigations on FGM beams under moving loads have been reported in the last two decades. Based on Rayleigh-Ritz method, Khalili *et al.* [9] constructed the discrete equation of motion for an Euler-Bernoulli beam under a moving mass, then used the differential quadrature method to compute the dynamic behavior of the beam. Rajabi *et al.* [10] analyzed the forced vibration of a FGM simply supported Euler-Bernoulli beam under a moving oscillator with the aid of the Petrov-Galerkin method. Gan *et al.* [11] studied dynamic response of FGM Timoshenko beam with material properties varying along the beam length using an element formulation. Dynamic analysis of FGM beams under moving loads was carried out by Şimşek and co-workers [12, 13] using a semi-analytical method. Ritz method was used in combination with Newmark method Songsowan *et al.* [14] in computing dynamic responses of FGSW Timoshenko beams resting on Pasternak foundation under a moving harmonic load.

In the above discussed references, the material properties of the beam change in only one direction, the transverse or axial direction. Development of beams with material properties varying in two or more directions plays an important role in practice. Several models for two-dimensional FGM (2D-FGM) and FGSW (2D-FGSW) beam and their mechanical behavior have been considered recently. Hao and Wei [15] assumed the beam material properties varying in both the beam thickness and length according to the exponential law in their free vibration study of 2D-FGM Timoshenko beams. Nguyen *et al.* [16] derived a finite element formulation for studying vibration of the 2D-FGM Timoshenko beam due to a moving load. The beam was considered to be formed from four materials with volume fraction varying in the thickness and length by power-law functions. Based on the NURBS method, Huynh *et al.* [17] investigated free vibration of 2D-FGM Timoshenko beams. Bending behavior of the 2D-FGSW beam was considered by Karamanli [18] using a quasi-3D shear deformation theory and symmetric smoothed particle hydrodynamics method.

In this paper, vibration of a 2D-FGSW Timoshenko beam formed from three distinct materials traversed by a harmonic load is studied by the finite element method. The beam consists of three layers, a homogeneous core and two FGM skin layers with the material properties continuously varying in both the thickness and length directions by power functions. A finite element formulation, in which linear, quadratic and cubic polynomials are employed to interpolate the axial displacement, rotation and transverse displacement is derived and employed in the study. Using the formulation, the natural frequencies and dynamic response are evaluated for the beam with various boundary conditions. The effects of the material and loading parameters on the vibration characteristics of the beam are examined in detail and highlighted.

## 2. 2D-FGM SANDWICH BEAM

### 2.1. 2D-FGSW beam

A 2D-FGSW beam with rectangular cross section ( $bxh$ ) as depicted in Figure 1 is considered. The beam consists of three layers, a homogeneous core and two FGM face layers with material properties varying in both the length and thickness directions. In the figure, a Cartesian coordinate ( $x, y, z$ ) is chosen such that the  $x$ -axis is on the mid-plane of the beam and the  $z$ -axis is perpendicular to the mid-plane and it directs upward. Denoting  $z_0 = -h/2, z_3 = h/2, z_1, z_2$  are the vertical coordinates of the bottom and top surface, the interfaces of the layers, respectively. The beam is subjected to a moving harmonic load  $P\cos\Omega t$ , moving from the left end to the right end of the beam with a constant speed  $v$ .

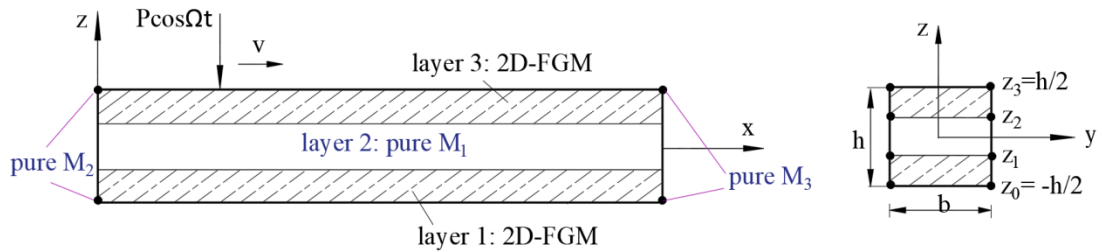


Figure 1. 2D-FGSW beam model in analysis of free and forced vibration.

The beam is assumed to be formed from three distinct materials, namely  $M_1, M_2$  and  $M_3$ . The volume fraction of  $M_1, M_2$  and  $M_3$  are assumed to vary in the  $x$  and  $z$  directions according to

$$\begin{cases}
 \text{for } z \in [z_0, z_1]: & \begin{cases}
 V_1^{(1)} = \left( \frac{z - z_0}{z_1 - z_0} \right)^{n_z}, \\
 V_2^{(1)} = \left[ 1 - \left( \frac{z - z_0}{z_1 - z_0} \right)^{n_z} \right] \left[ 1 - \left( \frac{x}{L} \right)^{n_x} \right], \\
 V_3^{(1)} = \left[ 1 - \left( \frac{z - z_0}{z_1 - z_0} \right)^{n_z} \right] \left( \frac{x}{L} \right)^{n_x},
 \end{cases} \\
 \text{for } z \in [z_1, z_2]: & V_1^{(2)} = 1, V_2^{(2)} = V_3^{(2)} = 0, \\
 \text{for } z \in [z_2, z_3]: & \begin{cases}
 V_1^{(3)} = \left( \frac{z - z_3}{z_2 - z_3} \right)^{n_z}, \\
 V_2^{(3)} = \left[ 1 - \left( \frac{z - z_3}{z_2 - z_3} \right)^{n_z} \right] \left[ 1 - \left( \frac{x}{L} \right)^{n_x} \right], \\
 V_3^{(3)} = \left[ 1 - \left( \frac{z - z_3}{z_2 - z_3} \right)^{n_z} \right] \left( \frac{x}{L} \right)^{n_x}
 \end{cases}
 \end{cases} \quad (1)$$

where  $V_1, V_2$  and  $V_3$  are, respectively, the volume fraction of the  $M_1, M_2$  and  $M_3$ ;  $L$  is total beam length;  $n_x$  and  $n_z$  are the grading indexes. The model defines a softcore sandwich beam if  $M_1$  is a

metal, and it is a hardcore one if  $M_1$  is a ceramic. Figure 2 shows the variation of  $V_1$ ,  $V_2$  and  $V_3$  of 2D-FGSW beam in the length and thickness directions for  $n_x=n_z=0.5$  and  $z_1=-h/5$ ,  $z_2=h/5$ .

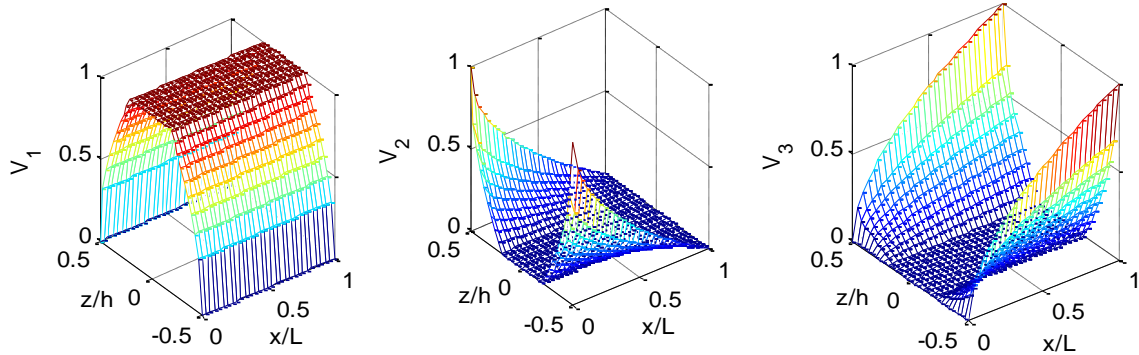


Figure 2. Variation of  $V_1$ ,  $V_2$  and  $V_3$  of the 2D-FGSW beam for  $n_x = n_z = 0.5$  and  $z_1 = -h/5$ ,  $z_2 = h/5$ .

The effective material properties  $P_f^{(k)}$ , such as the Young's modulus  $E_f^{(k)}$ , shear modulus  $G_f^{(k)}$  and mass density  $\rho_f^{(k)}$ , of the  $k$ th layer ( $k = 1..3$ ) evaluated by Voigt's model are of the form

$$P_f^{(k)} = P_1V_1^{(k)} + P_2V_2^{(k)} + P_3V_3^{(k)} \quad (2)$$

where  $P_1$ ,  $P_2$  and  $P_3$  represent the properties of the M1, M2 and M3, respectively. Substituting Eq. (1) into Eq. (2), one gets

$$\begin{cases} P_f^{(1)}(x, z) = [P_1 - P_{23}(x)] \left( \frac{z - z_0}{z_1 - z_0} \right)^{n_z} + P_{23}(x) & \text{for } z \in [z_0, z_1] \\ P_f^{(2)}(x, z) = P_1 & \text{for } z \in [z_1, z_2] \\ P_f^{(3)}(x, z) = [P_1 - P_{23}(x)] \left( \frac{z - z_3}{z_2 - z_3} \right)^{n_z} + P_{23}(x) & \text{for } z \in [z_2, z_3] \end{cases} \quad (3)$$

where

$$P_{23}(x) = P_2 - (P_2 - P_3) \left( \frac{x}{L} \right)^{n_x} \quad (4)$$

One can easily verify that if  $n_x = 0$  or  $M_2$  is identical to  $M_3$ , Eq. (3) reduces to the expression for the effective material properties of unidirectional FGSW beam made of  $M_1$  and  $M_3$  in [6]. Furthermore, if  $n_z = 0$ , Eq. (3) reduces to the property of a homogenous beam of  $M_1$ .

## 2.2. Basic equations

Based on the Timoshenko beam theory, the displacements of a point in  $x$  and  $z$  directions,  $u_1(x, z, t)$  and  $u_3(x, z, t)$ , respectively, can be written in the following matrix form

$$\begin{Bmatrix} u_1(x, z, t) \\ u_3(x, z, t) \end{Bmatrix} = \begin{bmatrix} 1 & -z & 0 \\ 0 & 0 & 1 \end{bmatrix} \begin{Bmatrix} u(x, t) \\ \theta(x, t) \\ w(x, t) \end{Bmatrix} \quad (5)$$

where  $u(x,t)$  and  $w(x,t)$  are the axial and transverse displacements of the point on the  $x$ -axis, respectively;  $\theta(x,t)$  is the rotation of the cross section;  $t$  is the time variable;  $z$  is the distance from the point to the  $z$ -axis.

Equation (5) leads to the axial strain  $\varepsilon_{xx}$  and shear strain  $\gamma_{xz}$  in the forms

$$\begin{Bmatrix} \varepsilon_{xx} \\ \gamma_{xz} \end{Bmatrix} = \begin{bmatrix} 1 & -z & 0 \\ 0 & 0 & 1 \end{bmatrix} \begin{Bmatrix} u_{,x} \\ \theta_{,x} \\ w_{,x} - \theta \end{Bmatrix} \quad (6)$$

where the subscript comma is used to denote the derivative with respect to the variable that follows.

The constitutive equation for the beam is of the form

$$\begin{Bmatrix} \sigma_{xx} \\ \tau_{xz} \end{Bmatrix} = \begin{bmatrix} E_f^{(k)}(x,z) & 0 \\ 0 & \psi G_f^{(k)}(x,z) \end{bmatrix} \begin{Bmatrix} \varepsilon_{xx} \\ \gamma_{xz} \end{Bmatrix} \quad (7)$$

where  $\sigma_{xx}$  and  $\tau_{xz}$  are, respectively, the axial and shear stresses;  $E_f^{(k)}$  and  $G_f^{(k)}$  are the effective Young and shear moduli given by Eq. (3);  $\psi$  is the shear correction factor chosen by 5/6 for the beam with the rectangular cross section.

The strain energy  $U$  of the beam resulted from Eq. (6) and (7) is of the form

$$\begin{aligned} U &= \frac{1}{2} \int_0^L \int_A [\sigma_{xx} \quad \tau_{xz}] \{\varepsilon_{xx} \quad \gamma_{xz}\}^T dA dx \\ &= \frac{1}{2} \int_0^L \{u_{,x} \quad \theta_{,x} \quad (w_{,x} - \theta)\} \begin{bmatrix} A_{11} & -A_{12} & 0 \\ -A_{12} & A_{22} & 0 \\ 0 & 0 & \psi A_{33} \end{bmatrix} \begin{Bmatrix} u_{,x} \\ \theta_{,x} \\ (w_{,x} - \theta) \end{Bmatrix} dx \end{aligned} \quad (8)$$

where  $A$  is the cross-sectional area;  $A_{11}, A_{12}, A_{22}$  and  $A_{33}$  are the beam rigidities, defined as

$$(A_{11}, A_{12}, A_{22}) = b \sum_{k=1}^3 \int_{z_{k-1}}^{z_k} E_f^{(k)}(x,z) (1, z, z^2) dz, \quad A_{33} = b \sum_{k=1}^3 \int_{z_{k-1}}^{z_k} G_f^{(k)}(x,z) dz \quad (9)$$

Substituting  $E_f^{(k)}(x,z)$  and  $G_f^{(k)}(x,z)$  from Eq. (3) into Eq. (9), one gets

$$A_{ij} = A_{ij}^{M_1} + A_{ij}^{M_2} + A_{ij}^{M_1 M_2} - A_{ij}^{M_2 M_3} \left(\frac{x}{L}\right)^{n_x}, \quad (i, j = 1..3) \quad (10)$$

with  $A_{ij}^{M_1}, A_{ij}^{M_2}, A_{ij}^{M_1 M_2}$  and  $A_{ij}^{M_2 M_3}$  are the rigidities contributed from  $M_1, M_2, M_1$  and  $M_2$  coupling,  $M_2$  and  $M_3$  coupling, respectively.

The kinetic energy  $T$  resulted from Eq. (5) is of the form

$$T = \frac{1}{2} \int_0^L \int_A \rho_f^{(k)}(x,z) \begin{bmatrix} \dot{u}_1 \\ \dot{u}_3 \end{bmatrix} dA dx = \frac{1}{2} \int_0^L \begin{bmatrix} \dot{u} & \dot{\theta} & \dot{w} \end{bmatrix} \begin{bmatrix} I_{11} & -I_{12} & 0 \\ -I_{12} & I_{22} & 0 \\ 0 & 0 & I_{11} \end{bmatrix} \begin{bmatrix} \dot{u} \\ \dot{\theta} \\ \dot{w} \end{bmatrix} dx \quad (11)$$

where the dot over a variable denotes the derivative of the variable with respect to time variable  $t$ ;  $\rho_f^{(k)}(x, z)$  are the effective mass density defined by Eq. (3);  $I_{11}, I_{12}$  and  $I_{22}$  are the mass moments, defined as

$$(I_{11}, I_{12}, I_{22}) = b \sum_{k=1}^3 \int_{z_{k-1}}^{z_k} \rho_f^{(k)}(x, z)(1, z, z^2) dz \tag{12}$$

As the rigidities, the mass moments can also be written in the following form

$$I_{ij} = I_{ij}^{M_1} + I_{ij}^{M_2} + I_{ij}^{M_1 M_2} - I_{ij}^{M_2 M_3} \left(\frac{x}{L}\right)^{n_x}, \quad (i, j = 1..3) \tag{13}$$

The potential of the load  $P \cos \Omega t$  is given by

$$V = - \int_0^L P \cos \Omega t w(x, t) \delta(x - vt) dx \tag{14}$$

where  $\delta(\cdot)$  is the Dirac delta function;  $x$  is the abscissa measured from the left end of the beam.

### 3. FINITE ELEMENT FORMULATION

The differential equation of motion for the beam can be obtained by applying Hamilton's principle to Eqs. (8), (11) and (14). However, as seen from Eqs. (10) and (13) that the beam rigidities and mass moments depend on  $x$ , thus it is difficult to obtain a closed-form solution for such differential equation. Therefore, a finite element formulation is derived herein for vibration analysis of the beam. Assuming the beam is divided into a number of two-node beam elements with length  $l$ . The vector of nodal displacements ( $\mathbf{d}$ ) contains six components as

$$\mathbf{d} = \{u_i \ w_i \ \theta_i \ u_j \ w_j \ \theta_j\}^T, \tag{15}$$

where  $u_i, w_i$  and  $\theta_i$  are, respectively, the values of the axial, transverse displacements and rotation  $\theta$  at the node  $i$ ;  $u_j, w_j$  and  $\theta_j$  are the corresponding quantities at the node  $j$ ; a superscript ' $T$ ' denotes the transpose of a vector or a matrix.

The displacement field  $\mathbf{u} = \{u \ \theta \ w\}^T$  are interpolated from their nodal values according to

$$\mathbf{u} = \mathbf{N} \mathbf{d} \tag{16}$$

where  $\mathbf{N}$  is the matrix of interpolation functions with the following form

$$\mathbf{N} = \begin{bmatrix} \mathbf{N}_u \\ \mathbf{N}_\theta \\ \mathbf{N}_w \end{bmatrix} = \begin{bmatrix} N_{u1} & 0 & 0 & N_{u2} & 0 & 0 \\ 0 & N_{\theta 1} & N_{\theta 2} & 0 & N_{\theta 3} & N_{\theta 4} \\ 0 & N_{w1} & N_{w2} & 0 & N_{w3} & N_{w4} \end{bmatrix} \tag{17}$$

The following polynomials are used as the interpolation functions herein

$$N_{u1} = \frac{l-x}{l}, \quad N_{u2} = \frac{x}{l} \tag{18}$$

$$\begin{aligned}
 N_{w1} &= \frac{1}{(1+\phi)} \left[ 2\left(\frac{x}{l}\right)^3 - 3\left(\frac{x}{l}\right)^2 - \phi\left(\frac{x}{l}\right) + (1+\phi) \right] \\
 N_{w2} &= \frac{l}{(1+\phi)} \left[ \left(\frac{x}{l}\right)^3 - \left(2 + \frac{\phi}{2}\right)\left(\frac{x}{l}\right)^2 + \left(1 + \frac{\phi}{2}\right)\left(\frac{x}{l}\right) \right]
 \end{aligned} \tag{19}$$

$$\begin{aligned}
 N_{w3} &= -\frac{1}{(1+\phi)} \left[ 2\left(\frac{x}{l}\right)^3 - 3\left(\frac{x}{l}\right)^2 - \phi\left(\frac{x}{l}\right) \right] \\
 N_{w4} &= \frac{l}{(1+\phi)} \left[ \left(\frac{x}{l}\right)^3 - \left(1 - \frac{\phi}{2}\right)\left(\frac{x}{l}\right)^2 - \frac{\phi}{2}\left(\frac{x}{l}\right) \right]
 \end{aligned}$$

$$\begin{aligned}
 N_{\theta 1} &= \frac{6}{(1+\phi)l} \left[ \left(\frac{x}{l}\right)^2 - \left(\frac{x}{l}\right) \right], & N_{\theta 2} &= \frac{1}{(1+\phi)} \left[ 3\left(\frac{x}{l}\right)^2 - (4+\phi)\left(\frac{x}{l}\right) + (1+\phi) \right] \\
 N_{\theta 3} &= -\frac{6}{(1+\phi)l} \left[ \left(\frac{x}{l}\right)^2 - \left(\frac{x}{l}\right) \right], & N_{\theta 4} &= \frac{1}{(1+\phi)} \left[ 3\left(\frac{x}{l}\right)^2 - (2-\phi)\left(\frac{x}{l}\right) \right]
 \end{aligned} \tag{20}$$

with  $\phi = 12A_{22} / (l^2 \psi A_{33})$ . The polynomials in Eq. (19) and (20) are previously derived by Kosmatka in [19] for a homogeneous Timoshenko beam element.

Using Eq. (16) and (17), the strain energy in Eq. (8) can be written in the form

$$\begin{aligned}
 U &= \frac{1}{2} \sum^{NE} \mathbf{d}^T \left\{ \int_0^l \begin{bmatrix} \mathbf{N}_{u,x}^T & \mathbf{N}_{\theta,x}^T & (\mathbf{N}_{w,x} - \mathbf{N}_{\theta})^T \end{bmatrix} \begin{bmatrix} A_{11} & -A_{12} & 0 \\ -A_{12} & A_{22} & 0 \\ 0 & 0 & \psi A_{33} \end{bmatrix} \begin{bmatrix} \mathbf{N}_{u,x} \\ \mathbf{N}_{\theta,x} \\ \mathbf{N}_{w,x} - \mathbf{N}_{\theta} \end{bmatrix} dx \right\} \mathbf{d} \\
 &= \frac{1}{2} \sum^{NE} \mathbf{d}^T (\mathbf{k}_{uu} - \mathbf{k}_{u\theta} + \mathbf{k}_{\theta\theta} + \mathbf{k}_{ss}) \mathbf{d}
 \end{aligned} \tag{21}$$

where NE is the total number of elements discretized the beam;  $\mathbf{k}_{uu}$ ,  $\mathbf{k}_{u\theta}$ ,  $\mathbf{k}_{\theta\theta}$  and  $\mathbf{k}_{ss}$  are, respectively, the element stiffness matrices stemming from the axial stretching, axial-bending coupling, bending and shear deformation, and they have the following forms

$$\begin{aligned}
 \mathbf{k}_{uu} &= \int_0^l \mathbf{N}_{u,x}^T A_{11} \mathbf{N}_{u,x} dx, & \mathbf{k}_{u\theta} &= \int_0^l \left[ \mathbf{N}_{u,x}^T A_{12} \mathbf{N}_{\theta,x} + \mathbf{N}_{\theta,x}^T A_{12} \mathbf{N}_{u,x} \right] dx \\
 \mathbf{k}_{\theta\theta} &= \int_0^l \mathbf{N}_{\theta,x}^T A_{22} \mathbf{N}_{\theta,x} dx, & \mathbf{k}_{ss} &= \int_0^l (\mathbf{N}_{w,x} - \mathbf{N}_{\theta})^T \psi A_{33} (\mathbf{N}_{w,x} - \mathbf{N}_{\theta}) dx
 \end{aligned} \tag{22}$$

The kinetic energy in Eq. (11) resulted from Eq. (16) and (17) is of the form

$$\begin{aligned}
 T &= \frac{1}{2} \sum^{NE} \dot{\mathbf{d}}^T \left\{ \int_0^l \begin{bmatrix} \mathbf{N}_u^T & \mathbf{N}_{\theta}^T & \mathbf{N}_w^T \end{bmatrix} \begin{bmatrix} I_{11} & -I_{12} & 0 \\ -I_{12} & I_{22} & 0 \\ 0 & 0 & I_{11} \end{bmatrix} \begin{bmatrix} \mathbf{N}_u \\ \mathbf{N}_{\theta} \\ \mathbf{N}_w \end{bmatrix} dx \right\} \dot{\mathbf{d}} \\
 &= \frac{1}{2} \sum^{NE} \dot{\mathbf{d}}^T (\mathbf{m}_{uu} + \mathbf{m}_{ww} - \mathbf{m}_{u\theta} + \mathbf{m}_{\theta\theta}) \dot{\mathbf{d}}
 \end{aligned} \tag{23}$$

with

$$\begin{aligned} \mathbf{m}_{uu} &= \int_0^l \mathbf{N}_u^T I_{11} \mathbf{N}_u dx, & \mathbf{m}_{ww} &= \int_0^l \mathbf{N}_w^T I_{11} \mathbf{N}_w dx \\ \mathbf{m}_{\theta\theta} &= \int_0^l \mathbf{N}_\theta^T I_{22} \mathbf{N}_\theta dx, & \mathbf{m}_{u\theta} &= \int_0^l [\mathbf{N}_u^T I_{12} \mathbf{N}_\theta + \mathbf{N}_\theta^T I_{12} \mathbf{N}_u] dx \end{aligned} \quad (24)$$

where  $\mathbf{m}_{uu}$ ,  $\mathbf{m}_{ww}$ ,  $\mathbf{m}_{u\theta}$  and  $\mathbf{m}_{\theta\theta}$  are the element mass matrices resulted from the axial and transverse translations, axial translation-rotation coupling, and cross-sectional rotation, respectively.

The equation of motion for analyzing vibration of the beam can be written as

$$\mathbf{M}\ddot{\mathbf{D}} + \mathbf{K}\mathbf{D} = \mathbf{F}_{\text{ex}} \quad (25)$$

where  $\mathbf{M}$  and  $\mathbf{K}$  are, respectively, the global mass and stiffness matrix of the beam;  $\ddot{\mathbf{D}}$  and  $\mathbf{D}$  are the vectors of global nodal acceleration and displacement, respectively;  $\mathbf{F}_{\text{ex}}$  is the vector of nodal external force which has the following form

$$\mathbf{F}_{\text{ex}} = \sum^{\text{NE}} \mathbf{f}_{\text{ex}}, \quad \text{with} \quad \mathbf{f}_{\text{ex}} = P \cos \Omega t \mathbf{N}_w^T \Big|_{x_e} \quad (26)$$

Noting that except for the element under loading, the element nodal force vector  $\mathbf{f}_{\text{ex}}$  is zero for all other elements. The notation  $\mathbf{N}_w^T \Big|_{x_e}$  means that the matrix of interpolation function  $\mathbf{N}_w^T$  are evaluated at the abscissa  $x_e$ , the current position of the moving load with respect to the left node of the element. Eq. (25) can be solved by the direct integration Newmark method. The average acceleration method which ensures the numerical instability of the method is adopted herein.

Setting the right hand side of Eq. (25) to zeros leads to equation for free vibration analysis as

$$\mathbf{M}\ddot{\mathbf{D}} + \mathbf{K}\mathbf{D} = \mathbf{0} \quad (27)$$

Assuming the vector of nodal displacements is in the harmonic form, Eq. (27) leads to an eigenvalue problem for determining the frequency  $\omega$  as

$$(\mathbf{K} - \omega^2 \mathbf{M})\bar{\mathbf{D}} = \mathbf{0} \quad (28)$$

where  $\bar{\mathbf{D}}$  is the vibration amplitude.

#### 4. NUMERICAL INVESTIGATION

A hardcore beam made from alumina ( $\text{Al}_2\text{O}_3$ ) as  $M_1$ , zirconia ( $\text{ZrO}_2$ ) as  $M_2$  and aluminum (Al) as  $M_3$  is used for numerical investigation in this section. The material properties of the constituents adopted from [6] are given in Table 1.

*Table 1.* Properties of constituent materials of 2D-FGSW beam.

| Materials                           | Role  | $E$ (GPa) | $\rho$ (kg/m <sup>3</sup> ) | $\nu$ |
|-------------------------------------|-------|-----------|-----------------------------|-------|
| Alumina ( $\text{Al}_2\text{O}_3$ ) | $M_1$ | 380       | 3960                        | 0.3   |
| Zirconia ( $\text{ZrO}_2$ )         | $M_2$ | 151       | 3000                        | 0.3   |
| Aluminum (Al)                       | $M_3$ | 70        | 2702                        | 0.3   |

The data for computations are as follows:  $b = 1$  m,  $h = 1$ ,  $P = 500$  kN. The following dimensionless parameters are introduced for natural frequencies and dynamic magnification factor (DMF)

$$\mu_i = \omega_i \frac{L^2}{h} \sqrt{\frac{\rho_{Al}}{E_{Al}}}, \text{ DMF} = \max\left(\frac{w(L/2, t)}{w_{st}}\right) \quad (29)$$

where  $\omega_i$  is the  $i$ th natural frequency, and  $w_{st} = PL^3/48E_z I$  is the static deflection of a simply supported zirconia beam under load, acting at the mid-span of the beam [14].

#### 4.1. Formulation verification

The accuracy and convergence of the derived formulation is firstly verified. Since there are no data on the beam model herein, the verification is carried out for the special case of 2D-FGSW beam when  $M_2$  is identical to  $M_3$ . In this case, the 2D-FGSW beam returns to a unidirectional FGSW beam made from  $Al_2O_3$  and Al, previously studied by Vo *et al.* in [6], and Songsuwan *et al.* in [14].

Table 2. Comparison of fundamental frequency parameter  $\mu_1$  of simply supported unidirectional FGSW beam with  $n_x = 0$  and  $L/h = 5$ .

| $n_z$ | Source  | 1-0-1  | 2-1-2  | 2-1-1  | 1-1-1  | 2-2-1  | 1-2-1  | 1-8-1  |
|-------|---------|--------|--------|--------|--------|--------|--------|--------|
| 0.5   | Ref.[6] | 4.1268 | 4.2351 | 4.2945 | 4.3303 | 4.4051 | 4.4798 | 4.8422 |
|       | Present | 4.1244 | 4.2305 | 4.3055 | 4.3253 | 4.4124 | 4.4754 | 4.8411 |
| 1     | Ref.[6] | 3.5735 | 3.7298 | 3.8187 | 3.8755 | 3.9896 | 4.1105 | 4.6795 |
|       | Present | 3.5595 | 3.7161 | 3.8438 | 3.8630 | 4.0077 | 4.1005 | 4.6764 |
| 10    | Ref.[6] | 2.6932 | 2.7355 | 2.8669 | 2.8808 | 3.0588 | 3.2356 | 4.2776 |
|       | Present | 2.6752 | 2.7191 | 2.9634 | 2.8668 | 3.1509 | 3.2240 | 4.2727 |

Table 3. Convergence of the element in evaluating fundamental frequency parameter of SS beam.

| Beam    | $n_x$ | $n_z$ | NE = 12 | NE = 14 | NE = 16 | NE = 18 | NE = 20 | NE = 22 | NE = 24 |        |
|---------|-------|-------|---------|---------|---------|---------|---------|---------|---------|--------|
| (2-2-1) | 3     | 0.5   | 4.8376  | 4.8375  | 4.8374  | 4.8374  | 4.8374  | 4.8374  | 4.8374  | 4.8374 |
|         |       | 1     | 4.5230  | 4.5229  | 4.5228  | 4.5227  | 4.5227  | 4.5227  | 4.5227  | 4.5227 |
|         |       | 2     | 4.2382  | 4.2381  | 4.2379  | 4.2378  | 4.2378  | 4.2378  | 4.2378  | 4.2378 |
|         |       | 5     | 4.0117  | 4.0114  | 4.0113  | 4.0111  | 4.0110  | 4.0110  | 4.0110  | 4.0110 |
| (2-1-2) | 3     | 0.5   | 4.6962  | 4.6961  | 4.6961  | 4.6960  | 4.6960  | 4.6960  | 4.6960  | 4.6960 |
|         |       | 1     | 4.3120  | 4.3119  | 4.3118  | 4.3118  | 4.3117  | 4.3117  | 4.3117  | 4.3117 |
|         |       | 2     | 3.9789  | 3.9787  | 3.9786  | 3.9785  | 3.9785  | 3.9785  | 3.9785  | 3.9785 |
|         |       | 5     | 3.7486  | 3.7484  | 3.7483  | 3.7483  | 3.7482  | 3.7481  | 3.7481  | 3.7481 |

Table 2 compares the fundamental frequency parameters of the unidirectional FGSW beam with  $L/h = 5$  obtained herein with the result of Ref. [6] where a refined shear deformation based finite element model was used. Regardless of the material indexes, the layer thickness ratio, a good agreement between the result of the present work with that of Ref. [6] is seen from Table 2.

The convergence of the derived element is shown in Table 3, where the fundamental frequency parameters of the SS beam with  $L/h = 20$  obtained by different number of the elements are given for various grading indexes and layer thickness ratios. As seen from the table 3, the 2D-FGSW beam needs 22 elements to achieve the convergence. Because of this convergence result, a mesh of 22 elements is used in all the computations reported below.

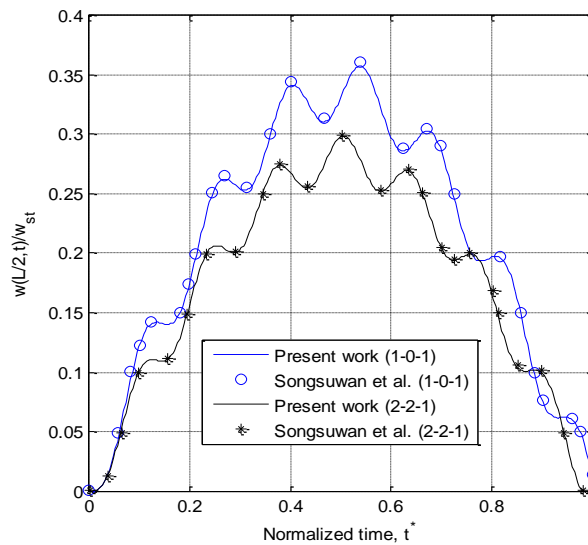


Figure 3. Comparison time histories for mid-span deflection of unidirectional FGM sandwich beam under a constant speed moving load ( $L/h = 10$ ,  $n_x = 0$ ,  $n_z = 0.5$ ,  $v = 50$  m/s).

Figure 3 compares the time histories for mid-span deflection of the unidirectional FGSW beam with  $b = 0.5$  m,  $h = 1.0$  m of the present work with the result of Songsuwan *et al.* in [14] for two layer thickness ratios, (1-0-1) and (2-2-1). Very good agreement between the present result with that of Ref. [14] is seen from Figure 3. Noting that the static deflection  $w_{st}$  in Figure 3 is the mid-span static deflection of the simply supported aluminum beam.

#### 4.2. Free vibration

Two types of boundary conditions, namely simply supported (SS) and clamped at both ends (CC) are considered herewith. The fundamental frequency parameters of the 2D-FGSW beam with an aspect ratio  $L/h = 20$  are given in Table 4 for the SS beams. As seen from the table, the frequency parameter decreases by increasing the grading index  $n_z$ , but it increases by increase of the grading index  $n_x$ , irrespective of the layer thickness ratio. The dependence of the fundamental frequency parameter upon the material grading indexes can be explained by the change of the effective Young's modulus as can be seen from Eqs. (2) and (3). An increase of  $n_z$  leads to a decrease of  $Al_2O_3$  percentage. Since Young's modulus of  $Al_2O_3$  is much higher than that of  $ZrO_2$  and Al, and thus the effective modulus decreases which leads to the decrease of the beam rigidities. On the other hand, the increase of index  $n_z$  also leads to the decrease of the mass moments, but this decrease is much lower than that of the rigidities. As a result, the fundamental frequency parameters decrease by increasing  $n_z$ . The increase of the frequency parameters by increasing  $n_x$  can be explained similarly.

In addition to the material grading indexes, Table 4 also shows an important role of the layer thickness ratio on the fundamental frequency parameters of the 2D-FGSW beam. The beam with a larger core thickness has a larger frequency parameter, regardless of the grading indexes. The variation of the frequency parameters  $\mu_i$  with the material grading indexes can also be seen from Figure 4, where the first four frequency parameters of the (2-1-2) SS beam are depicted for an aspect ratio  $L/h = 20$ . The dependence of the higher frequency parameters upon

the grading indexes is similar to that of the fundamental frequency parameter. All the frequency parameters increase by decreasing index  $n_z$  and it decreases by increasing index  $n_x$ .

Table 4. Fundamental frequency parameter of SS beam for various grading indexes and layer thickness ratios ( $L/h = 20$ ).

| $n_x$ | $n_z$ | 1-0-1  | 2-1-2  | 2-1-1  | 1-1-1  | 2-2-1  | 1-2-1  | 1-8-1  |
|-------|-------|--------|--------|--------|--------|--------|--------|--------|
| 0.5   | 0     | 5.4603 | 5.4603 | 5.4603 | 5.4603 | 5.4603 | 5.4603 | 5.4603 |
|       | 0.3   | 4.7691 | 4.8354 | 4.8833 | 4.8959 | 4.9522 | 4.9934 | 5.2401 |
|       | 0.5   | 4.4379 | 4.5349 | 4.6089 | 4.6248 | 4.7108 | 4.7707 | 5.1379 |
|       | 1     | 3.9090 | 4.0442 | 4.1658 | 4.1780 | 4.3168 | 4.4019 | 4.9698 |
|       | 5     | 3.2080 | 3.2596 | 3.4690 | 3.3981 | 3.6372 | 3.7109 | 4.6383 |
| 1     | 0     | 5.4603 | 5.4603 | 5.4603 | 5.4603 | 5.4603 | 5.4603 | 5.4603 |
|       | 0.3   | 4.8130 | 4.8743 | 4.9190 | 4.9305 | 4.9831 | 5.0215 | 5.2528 |
|       | 0.5   | 4.5068 | 4.5955 | 4.6641 | 4.6783 | 4.7582 | 4.8136 | 5.1567 |
|       | 1     | 4.0248 | 4.1452 | 4.2570 | 4.2664 | 4.3942 | 4.4715 | 4.9992 |
|       | 5     | 3.4108 | 3.4461 | 3.6333 | 3.5639 | 3.7788 | 3.8408 | 4.6898 |
| 5     | 0     | 5.4603 | 5.4603 | 5.4603 | 5.4603 | 5.4603 | 5.4603 | 5.4603 |
|       | 0.3   | 4.9074 | 4.9581 | 4.9961 | 5.0051 | 5.0499 | 5.0821 | 5.2803 |
|       | 0.5   | 4.6541 | 4.7253 | 4.7828 | 4.7932 | 4.8604 | 4.9059 | 5.1975 |
|       | 1     | 4.2700 | 4.3601 | 4.4513 | 4.4551 | 4.5600 | 4.6208 | 5.0626 |
|       | 5     | 3.8306 | 3.8356 | 3.9775 | 3.9126 | 4.0780 | 4.1163 | 4.8008 |

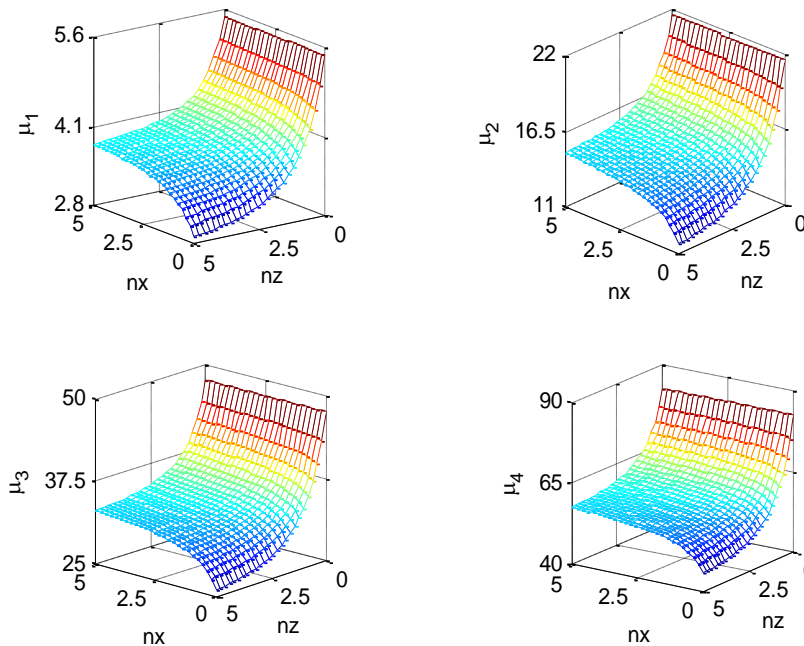


Figure 4. Variation of the first four frequency parameters with grading indexes of (2-1-2) SS beam.

The effect of the aspect ratio  $L/h$  on the fundamental frequency parameter  $\mu_1$  of the 2D-FGSW beam is illustrated in Figure 5 for the SS and CC beams with  $n_x = n_z = 2$  and various layer thickness ratios. As seen from the figure, the frequency parameter  $\mu_1$  increases by increasing the aspect ratio, regardless of layer thickness ratio and the boundary conditions. The influence of the

layer thickness ratio on the frequency parameter can be seen again from Figure 5, and the frequency parameter is higher for the beam having a larger core thickness, regardless of the boundary conditions.

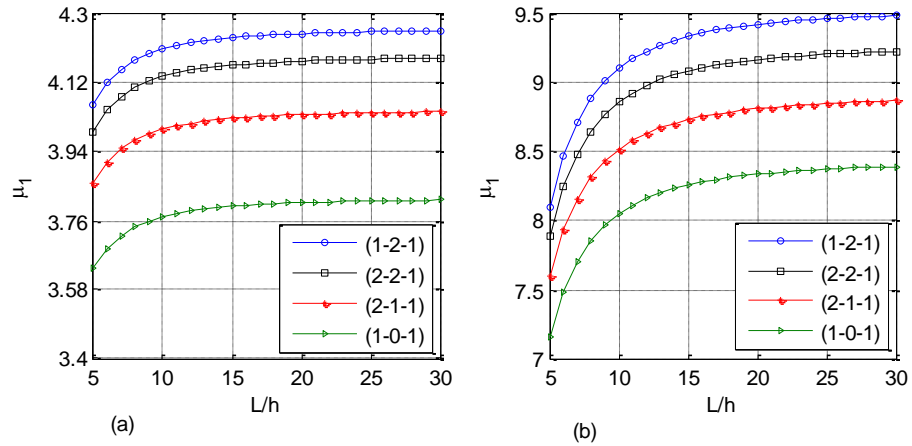


Figure 5. Effect of aspect ratio on fundamental frequency parameter of 2D-FGSW beam with  $n_x = n_z = 2$ :

(a) SS beam, (b) CC beam.

### 4.3. Forced vibration

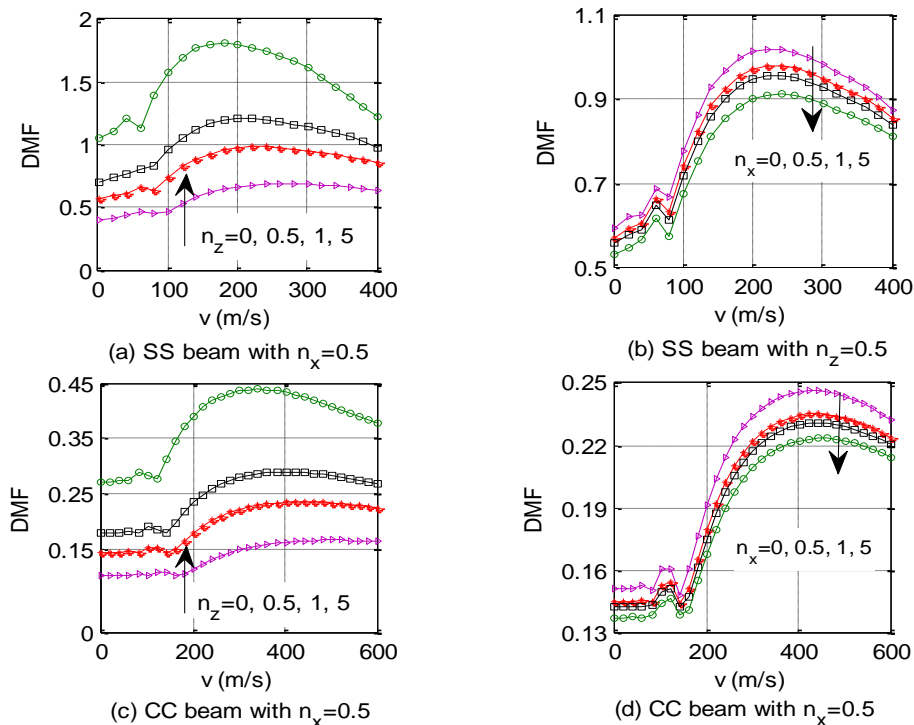


Figure 6. Variation of DMF of (2-2-1) beam for various moving load speed ( $\Omega = 0, L/h = 20$ ).

The dynamic behavior of the SS and CC beams with  $L/h = 20$  traversed by the moving harmonic load is examined in this sub-section. It is assumed that the moving harmonic speed  $v$  is

constant herein. The effects of the moving load speed and the material grading indexes on the DMF are shown Figure 6 for the (2-2-1) beam and  $\Omega = 0$ . The DMF, as seen from the figure, is significantly influenced by the moving load speed and the material grading indexes. The DMF increases by the increase of the index  $n_z$ , and it decreases by increasing index  $n_x$ . The DMF firstly increases by increasing the moving load speed, and then it reaches a maximum value before decreasing. The moving load speed at which the DMF attains the maximum value clearly depend on the grading index. In addition, the moving load speed corresponding to the maximum DMF of the CC beam is much larger comparing to the SS beam.

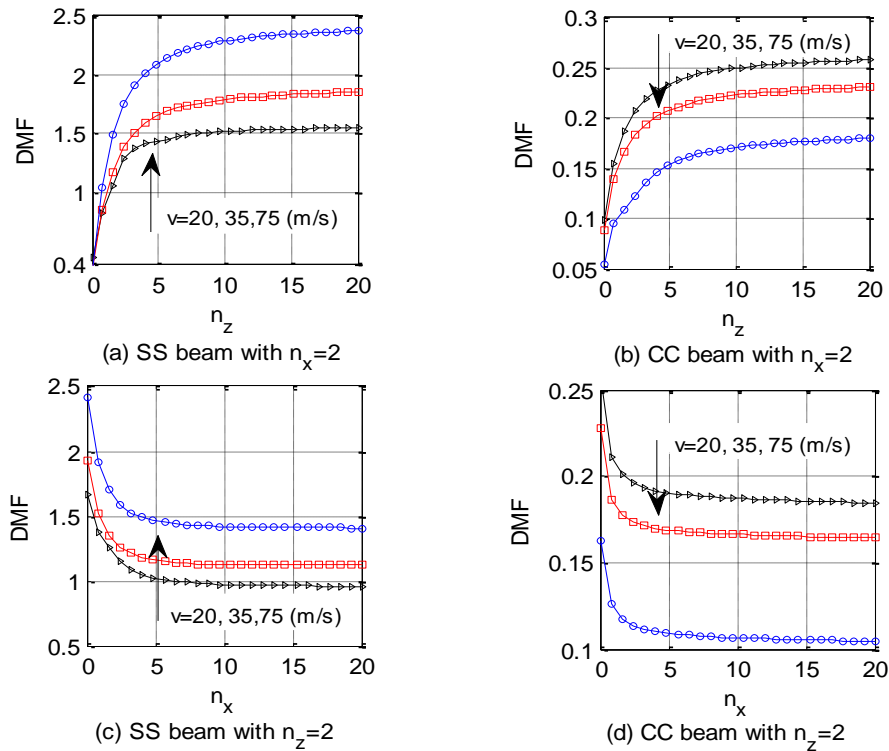


Figure 7. Variation of DMF of (2-2-1) beam with the grading index for various moving harmonic load speed  $\Omega = 30$  rad/s.

Figure 7 shows the variation of the DMF with the material grading indexes of the SS and CC beams for an excitation frequency  $\Omega = 30$  rad/s and three values of the moving load speed,  $v = 20$  m/s,  $v = 35$  m/s and  $v = 75$  m/s. The dependence of the DMF as remarked above is clearly seen from the figure again. The influence of the moving load speed on the DMF of the SS beam is different from that of the CC when  $n_z = 2$ . Though the dependence of DMF on  $n_x$  of the two beams is the same, the increase of the moving load speed leads to an increase of the DMF of the SS beam, but it leads to a decrease of the DMF of the CC beam.

The relation between the DMF and the excitation frequency  $\Omega$  is shown in Figures 8 and 9 for the SS and CC beams, respectively. The DMF increases rapidly when the excitation frequency approaches the fundamental frequencies of the beams. The layer thickness ratio and the material grading indexes, as seen from the figures, alter the DMF. The change of the DMF due to the change of the layer thickness ratio is, however less significant than by the change of the index  $n_z$ , irrespective of the boundary conditions. This is due to the fact that the fundamental

frequency of the 2D-FGSW beam is influenced by the change of the index  $n_z$  more significantly than that by the layer thickness ratio. For example, the frequency  $\omega_1$  of the (1-0-1), (2-1-1) and (3-2-1) SS beam, with  $n_x = n_z = 0.5$ , is 56.4702 rad/s, 58.6462 rad/s and 59.9110 rad/s, respectively, and that of CC beam with the same layer thickness ratio is 127.3216 rad/s, 131.7258 rad/s, 134.1372 rad/s. On the other hand, the frequency of the (2-2-1) SS beam with  $(n_x, n_z) = (0.5, 0)$ ,  $(0.5, 0.5)$ ,  $(0.5, 3)$  is 69.4805 rad/s, 59.9432 rad/s, 48.1070 rad/s, respectively, and that of the CC beam is 155.4987 rad/s, 134.6120 rad/s, 107.5614 rad/s.

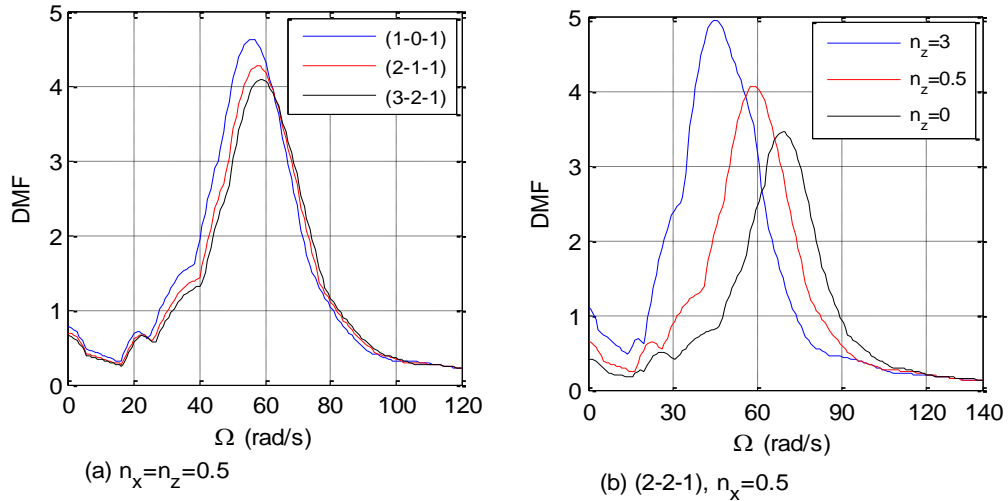


Figure 8. The DMF of the SS beam with moving harmonic load speed  $v=50$  m/s.

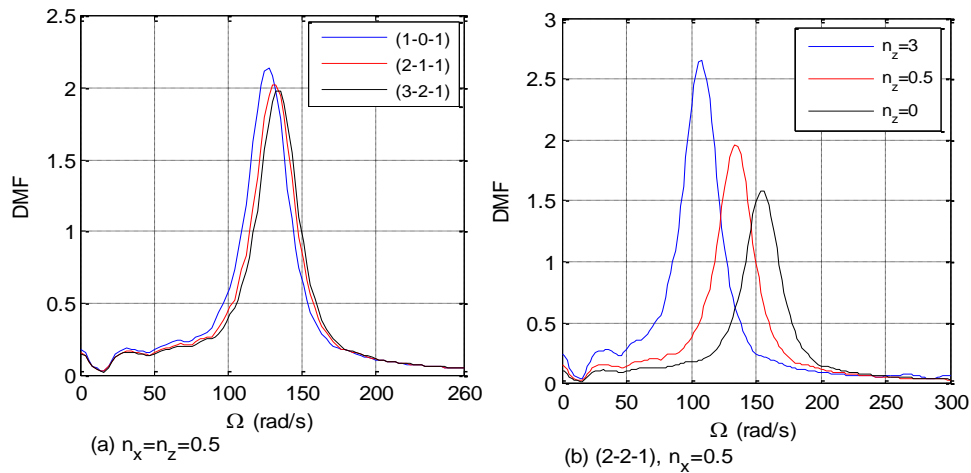


Figure 9. The DMF of the CC beam with moving harmonic load speed  $v = 50$  m/s.

To illustrate the influence of the excitation frequency and the material grading indexes on the DMF in some more further, Figure 10 shows the variation of the DMF of the (2-2-1) SS and CC beam with grading indexes for two values of the excitation frequency,  $\Omega = 25$  rad/s and  $\Omega = 35$  rad/s. As clearly seen from the figure, the DMF is higher for the beam under the moving load with the large excitation frequency, regardless of the material grading indexes and the boundary

condition. The difference between the DMF by the excitation frequency is more pronounced for the larger index  $n_z$  and smaller index  $n_x$ , regardless of the boundary conditions.

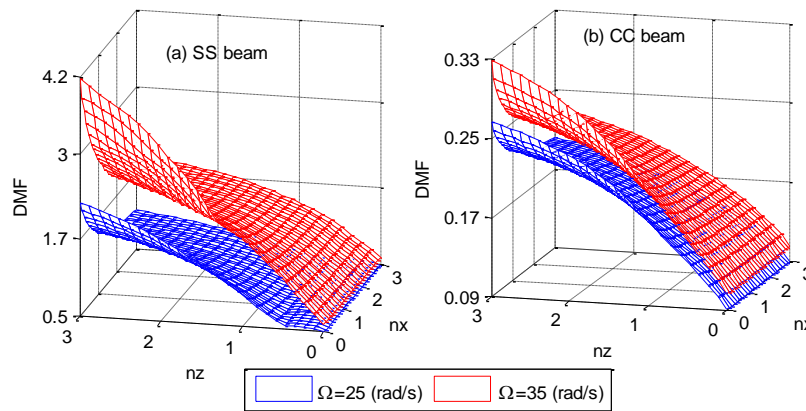


Figure 10. Variation of the DMF of the (2-2-1) beam with moving harmonic load speed  $v = 50$  m/s.

#### 4. CONCLUSIONS

Free and forced vibration of a 2D-FGSW Timoshenko beam traversed by a harmonic load has been studied by a finite element formulation. The beam formed from three distinct materials is assumed to consist of three layers, a homogeneous core and two FGM skin layers with the material properties continuously varying in both the thickness and length directions by the power functions. A finite element formulation was derived and employed to compute the natural frequencies and dynamic response of the beam. The accuracy of the formulation was confirmed through a comparison study. The obtained numerical results reveal that the material indexes, the layer thickness ratio, the excitation frequency and the moving load speed play an important role on the vibration characteristics of the beams. The influence of the aspect ratio on the vibration of the beam has also been examined and discussed.

#### REFERENCES

1. Koizumi M. - FGM activities in Japan, Compos. Part B: Eng. **28** (1-2) (1997) 1-4.
2. Sakiyama T., Matsuda H., and Morita C. - Free vibration analysis of sandwich beam with elastic or viscoelastic core by applying the discrete green function, J. Sound Vib. **191** (2) (1996) 189-206.
3. Apetre N.A., Sankar B.V. and Ambur D.R. - Analytical modeling of sandwich beams with functionally graded core, J. Sandw. Struct. Mater. **10** (1) (2008) 53-74.
4. Amirani M. C., Khalili S. M. R., and Nemati N. - Free vibration analysis of sandwich beam with FG core using the element free Galerkin method, Compos. Struct. **90** (2009) 373-379.
5. Rahmani O., Khalili S. M. R., Malekzadeh K., and Hadavinia H. - Free vibration analysis of sandwich structures with a flexible functionally graded syntactic core, Compos. Struct. **91** (2) (2009) 229-235.

6. Vo T. P., Thai H. T., Nguyen T. K., Maheri A., Lee J. - Finite element model for vibration and buckling of functionally graded sandwich beams based on a refined shear deformation theory, *Eng. Struct.* **64** (2014) 12–22.
7. Nguyen T. K., Nguyen B. D. - A new higher-order shear deformation theory for static, buckling and free vibration analysis of functionally graded sandwich beams, *J. Sandw. Struct. Mater.* **17** (2015) 1-19.
8. Vo T. P., Thai H. T., Nguyen T. K., Inam F., and Lee J. - A quasi-3D theory for vibration and buckling of functionally graded sandwich beams, *Compos. Struct.* **119** (2015) 1-12.
9. Khalili S. M. R., Jafari A. A., and Eftekhari S. A. - A mixed Ritz-DQ method for forced vibration of functionally graded beams carrying moving loads, *Compos. Struct.* **92** (10) (2010) 2497-2511.
10. Rajabi K., Kargarnovin M. H., and Gharini M. - Dynamic analysis of a functionally graded simply supported Euler-Bernoulli beam subjected to a moving oscillator, *Acta Mech.* **224** (2) (2013) 425-446.
11. Gan B. S., Trinh T. H., Le T. H., and Nguyen D. K. - Dynamic response of non-uniform Timoshenko beams made of axially FGM subjected to multiple moving point loads, *Struct. Eng. Mech.* **53** (5) (2015) 981-995.
12. Şimşek M., Kocatürk T., and Akbaş Ş. D. - Dynamic behavior of an axially functionally graded beam under action of a moving harmonic load, *Compos. Struct.* **94** (8) (2012) 2358-2364.
13. Şimşek M. and Al-shujairi M. - Static, free and forced vibration of functionally graded (FG) sandwich beams excited by two successive moving harmonic loads, *Compos. Part B: Eng.* **108** (2017) 18-34.
14. Songsuwan W., Pimsarn M., and Wattanasakulpong N. - Dynamic responses of functionally graded sandwich beams resting on elastic foundation under harmonic moving loads, *Int. J. Struct. Stab. Dynam.* **18** (9) (2018) 1850112.
15. Hao D. and Wei C. - Dynamic characteristics analysis of bi-directional functionally graded Timoshenko beams, *Compos. Struct.* **141** (2016) 253-263.
16. Nguyen D. K., Nguyen Q. H., Tran T. T., and Bui V. T. - Vibration of bi-dimensional functionally graded Timoshenko beams excited by a moving load, *Acta Mech.* **228** (1) (2017) 141-155.
17. Huynh T. A., Lieu X. Q., and Lee J. - NURBS-based modeling of bidirectional functionally graded, *Compos. Struct.* **160** (2017) 1178-1190.
18. Karamanli A. - Bending behaviour of two directional functionally graded sandwich beams by using a quasi-3D shear deformation theory, *Compos. Struct.* **174** (2017) 70–86.
19. Kosmatka J. B. - an improved two-node finite element for stability and natural frequencies of axial-loaded Timoshenko beams, *comput. Struct.* **57** (1) (1995) 141-149.